PHYSICAL REVIEW D **88,** 036012 (2013)

Shear viscosity in the Nambu–Jona-Lasinio model with Φ-derivable approximations

Wei-jie Fu*

Department of Physics, Brandon University, Brandon, Manitoba, R7A 6A9, Canada

(Received 26 April 2013; published 23 August 2013)

Within the Nambu–Jona-Lasinio model the temperature dependence of the shear viscosity is calculated to the first nontrivial order in the $1/N_c$ expansion with Φ-derivable approximations. The two-particle irreducible effective action is computed to next-to-leading order, from which the integral equations for the 3- and 4-point vertices are obtained. These sum infinite sets of diagrams contributing to the shear viscosity at the same order in the $1/N_c$ expansion. We find that the shear viscosity decreases rapidly when the chiral crossover is approached. Comparing with the hadron phase, the quark-gluon plasma phase has a low shear viscosity, which is consistent with the measurements. The ratio of the shear viscosity to entropy density is also calculated.

DOI: 10.1103/PhysRevD.88.036012 PACS numbers: 11.10.Wx, 11.15.Pg, 11.30.Rd, 12.38.Mh

I. INTRODUCTION

It is believed that a strongly interacting quark-gluon plasma (QGP, or sQGP) is observed in ultrarelativistic heavy ion collisions at the Relativistic Heavy-Ion Collider (RHIC) [1–8]. The collective behavior of the sQGP is almost like that of an ideal fluid, with a ratio of the shear viscosity to entropy density η/s very close to the Kovtun-Policastro-Son-Starinets (KPSS) lower bound $1/4\pi$ [9]. In fact, the extraction of the transport coefficients from flow measurements finds $1 < 4\pi(\eta/s) < 2.5$ near the critical temperature [10–12].

Motivated by the experimental studies of the transport properties of strong-interaction matter, theoretical predictions for the shear viscosity of the QGP have attracted much attention. Employing kinetic theory, transport coefficients were calculated in high temperature gauge theories in the weak-coupling expansion [13] and the large N_f limit [14]. Recently, the contribution of the $gg \leftrightarrow ggg$ process to the shear viscosity of a gluon plasma is discussed in perturbative QCD [15,16]. Transport coefficients are also calculated in a weakly coupled scalar field theory using field theoretical methods [17], in which an infinite class of diagrams contributing to the leading weak-coupling behavior is summed through an integral equation. Similar calculations were also performed in the real-time formalism [18]. It should be emphasized that these types of calculations rely on perturbative treatments of the system and become unreliable near the QCD (pseudo)critical temperature. A way to overcome this problem is to employ lattice simulations [19]. However, before lattice results become quantitatively reliable, one has to solve the problem of how to reliably perform the analytic continuation from imaginary to real time based on a discrete set of data points [20].

A quite different approach to calculate the shear viscosity is to adopt the AdS/CFT correspondence, where the strong-coupling limit in a conformal field theory is mapped onto the weak-coupling limit of a gravity dual with anti–de Sitter metric. Then the shear viscosity of the conformal field theory can be calculated from graviton absorption, and one obtains the lower bound $1/4\pi$ for the shear viscosity to entropy density ratio η/s [9]. This bound is modified by higher-derivative gravity corrections [21]. One should mention that it is doubted whether the lower bound is universal [22], and it is argued that quantum field theory appears to impose no lower bound on η/s, at least for metastable fluids [23].

In this work we will study the shear viscosity in the Nambu–Jona-Lasinio (NJL) model within a Φ-derivable approximation [24,25], which is also known as the two-particle-irreducible (2PI) effective action formalism [26] and is a nonperturbative approach to quantum field theory. The Φ-derivable approximation has also been widely used to study the thermodynamics of quantum fields [27], quantum dynamics far from equilibrium [28], and to formulate efficient nonperturbative approximation schemes combined with the exact renormalization group [29]. The shear viscosity in the $O(N)$ model has also been computed using Φ-derivable approximations [30]. Furthermore, in a scalar theory with cubic and quartic interactions, the four-loop four-particle irreducible effective action is studied [31]. The NJL model, as a low-energy effective field theory of the QCD, is very successful in describing the static properties of light hadrons and the chiral phase transition at finite temperature [32,33]. The NJL model incorporates chiral symmetry and its dynamical breaking mechanism in a similar way as QCD. It is therefore interesting to calculate the shear viscosity and study its evolution from low temperatures towards the chiral transition. For this one has to go beyond the leading-order mean-field approximation, in a symmetry-conserving fashion. A systematic scheme is provided by the $1/N_c$ expansion [34,35]. In this paper we will compute the shear viscosity at first nontrivial order in $1/N_c$.

The paper is organized as follows. In Sec. II we introduce the Φ-derivable approximation and derive the

*fuw@brandonu.ca

integral equation for the 4-point vertex formally. In Sec. III we study the meson propagators and quark self-energy in details. In Sec. IV we solve the integral equation for the 3-point vertex numerically and obtain the shear viscosity from the Kubo formula. Section V summarizes the results and draws pertinent conclusions.

II. Φ-DERIVABLE APPROXIMATIONS

We begin with the Lagrangian density for the two-flavor NJL model:

$$\mathcal{L}_{\mathrm{NJL}} = \bar{\psi}(i\gamma_\mu\partial^\mu - m_0)\psi + G[(\bar{\psi}\psi)^2 + (\bar{\psi}i\gamma_5\vec{\tau}\psi)^2], \tag{1}$$

where m_0 is a small bare quark mass and $\tau^a (a = 1, 2, 3)$ denote Pauli matrices in flavor space. The four-fermion interaction with effective coupling strength G for scalar and pseudoscalar channels has $SU_V(2) \times SU_A(2) \times U_V(1)$ symmetry, which is broken to $SU_V(2) \times U_V(1)$ in the nonperturbative vacuum.

The corresponding generating functional with a two-point source for the NJL Lagrangian is given as

$$Z[\eta, \bar{\eta}, K] = \int [d\psi][d\bar{\psi}] \exp\{i[I(\bar{\psi}, \psi) + \bar{\eta}\psi + \bar{\psi}\eta + \bar{\psi}K\psi]\}. \tag{2}$$

Here, $I(\bar{\psi}, \psi) = \int d^4x \mathcal{L}_{\mathrm{NJL}}$ is the classical action, and in the expression above we have used the following abbreviated notations:

$$\bar{\eta}\psi = \int d^4x \bar{\eta}(x)\psi(x), \qquad \bar{\psi}\eta = \int d^4x \bar{\psi}(x)\eta(x),$$
$$\bar{\psi}K\psi = \int d^4x d^4y \bar{\psi}(x)K(x, y)\psi(y). \tag{3}$$

Introducing the generating functional for the connected Green functions

$$W[\eta, \bar{\eta}, K] = -i \ln Z[\eta, \bar{\eta}, K], \tag{4}$$

it then follows that

$$\frac{\delta W[\eta, \bar{\eta}, K]}{\delta \bar{\eta}(x)} = \psi_c(x), \tag{5}$$

$$\frac{\delta W[\eta, \bar{\eta}, K]}{\delta \eta(x)} = -\bar{\psi}_c(x), \tag{6}$$

$$\frac{\delta W[\eta, \bar{\eta}, K]}{\delta K(y, x)} = -(\psi_c(x)\bar{\psi}_c(y) + iS(x, y)). \tag{7}$$

In the case of vanishing sources, $\psi_c(x)$ and $\bar{\psi}_c(x)$ become expectation values of the corresponding fields $\psi(x)$ and $\bar{\psi}(x)$, and $iS(x, y)$ is the propagator.

The generating functional for the vertex Green functions is defined as the Legendre transform of W

$$\Gamma[\psi_c, \bar{\psi}_c, S] = W[\eta, \bar{\eta}, K] - \bar{\eta}\psi_c - \bar{\psi}_c\eta + \mathrm{Tr}[K(\psi_c\bar{\psi}_c + iS)], \tag{8}$$

where

$$\mathrm{Tr}[K(\psi_c\bar{\psi}_c + iS)] = \int d^4x d^4y K(x, y)(\psi_c(y)\bar{\psi}_c(x) + iS(y, x)). \tag{9}$$

It can be easily proved that

$$\frac{\delta\Gamma[\psi_c, \bar{\psi}_c, S]}{\delta\psi_c(x)} = \bar{\eta}(x) + \int d^4y \bar{\psi}_c(y)K(y, x), \tag{10}$$

$$\frac{\delta\Gamma[\psi_c, \bar{\psi}_c, S]}{\delta\bar{\psi}_c(x)} = -\eta(x) - \int d^4y K(x, y)\psi_c(y), \tag{11}$$

$$\frac{\delta\Gamma[\psi_c, \bar{\psi}_c, S]}{\delta S(x, y)} = iK(y, x). \tag{12}$$

Using the Φ-derivable theory [24,25], the effective action Γ in Eq. (8) can be computed as follows:

$$\Gamma[\psi_c, \bar{\psi}_c, S] = I(\psi_c, \bar{\psi}_c) - i\mathrm{Tr}\ln S^{-1} - i\mathrm{Tr}S_0^{-1}(\psi_c, \bar{\psi}_c)S + \Gamma_2[\psi_c, \bar{\psi}_c, S] + \mathrm{const}, \tag{13}$$

where the $S_0^{-1}(\psi_c, \bar{\psi}_c)$ satisfies

$$\bar{\psi}S_0^{-1}(\psi_c, \bar{\psi}_c)\psi = \left(\bar{\psi}\frac{\delta}{\delta\bar{\psi}_c}\right)\left(\psi\frac{\delta}{\delta\psi_c}\right)I(\psi_c, \bar{\psi}_c), \tag{14}$$

and Γ_2 is the sum of 2PI vacuum graphs governed by vertices of $I_{\mathrm{int}}(\psi_c, \bar{\psi}_c; \psi, \bar{\psi})$ and the propagator iS [26]. Here $I_{\mathrm{int}}(\psi_c, \bar{\psi}_c; \psi, \bar{\psi})$ is given as

$$I_{\mathrm{int}}(\psi_c, \bar{\psi}_c; \psi, \bar{\psi}) = I(\psi + \psi_c, \bar{\psi} + \bar{\psi}_c) - I(\psi_c, \bar{\psi}_c) - \bar{\psi}\frac{\delta I(\psi_c, \bar{\psi}_c)}{\delta\bar{\psi}_c} - \psi\frac{\delta I(\psi_c, \bar{\psi}_c)}{\delta\psi_c} - \bar{\psi}S_0^{-1}(\psi_c, \bar{\psi}_c)\psi. \tag{15}$$

Since we are only interested in $\psi_c = \bar{\psi}_c = 0$, it then follows that

$$S_0^{-1}(x - y) = (i\gamma_\mu\partial^\mu - m_0)\delta^4(x - y), \tag{16}$$

$$I_{\mathrm{int}}(\psi, \bar{\psi}) = G[(\bar{\psi}\psi)^2 + (\bar{\psi}i\gamma_5\vec{\tau}\psi)^2]. \tag{17}$$

We should note that in Eqs. (15) and (17) we have used abbreviated notations, where the integrations are not indicated.

Using the 2PI formalism above, we can easily obtain an integral equation for the 4-point vertex function $\Gamma^{(4)}$. It follows from Eqs. (7) and (12) that

$$\frac{\partial^2\Gamma[S]}{\partial S_{ij}\partial S_{k'l'}}\frac{\partial^2 W[K]}{\partial K_{l'k'}\partial K_{lk}} = \mathbb{1}_{ij;kl}, \tag{18}$$

where $\mathbb{1}_{ij;kl} = \delta_{ik}\delta_{jl}$, $ij\ldots$ stands for all the degrees of freedom of the Dirac field and a summation is assumed in

the case of repeated indices. Here we use the ordinary differential ∂ in place of the functional differential δ. Employing Eq. (4) one obtains

$$\frac{\partial^2 W[K]}{\partial K_{l'k'}\partial K_{lk}} = i(\langle T(\psi_{k'}\bar{\psi}_{l'}\psi_k\bar{\psi}_l)\rangle_{\text{conn}} - \langle T(\psi_{k'}\bar{\psi}_l)\rangle\langle T(\psi_k\bar{\psi}_{l'})\rangle), \quad (19)$$

where the first term in the right-hand side is the connected 4-point Green function. The connected Green function can further be expressed as

$$\langle T(\psi_{k'}\bar{\psi}_{l'}\psi_k\bar{\psi}_l)\rangle_{\text{conn}} = (iS_{k'k_1})(iS_{l_1l'})(iS_{kk_2})(iS_{l_2l})\Gamma^{(4)}_{k_1l_1;k_2l_2}. \quad (20)$$

Differentiating $\Gamma[S]$ in Eq. (13) with respect to S, we arrive at

$$\frac{\partial\Gamma[S]}{\partial S_{ij}} = i(S^{-1})_{ji} - i(S_0^{-1})_{ji} + \frac{\partial\Gamma_2[S]}{\partial S_{ij}}. \quad (21)$$

Requiring stationarity, i.e. the left-hand side to vanish, the gap equation emerges:

$$S^{-1} = S_0^{-1} - \Sigma, \quad (22)$$

with

$$\Sigma = -i\frac{\partial\Gamma_2[S]}{\partial S}. \quad (23)$$

Differentiating both sides of Eq. (21) with respect to S once more, one obtains

$$\frac{\partial^2\Gamma[S]}{\partial S_{ij}\partial S_{k'l'}} = i(iS)^{-1}_{jk'}(iS)^{-1}_{l'i} + \frac{\partial^2\Gamma_2[S]}{\partial S_{ij}\partial S_{k'l'}}. \quad (24)$$

Substituting Eqs. (19), (20), and (24) into Eq. (18) one obtains the following integral equation for $\Gamma^{(4)}$:

$$\Gamma^{(4)}_{ij;kl} = \Lambda_{ij;kl} - \Lambda_{ij;k'l'}(iS_{l'i'})\Gamma^{(4)}_{i'j';kl}(iS_{j'k'}). \quad (25)$$

The scattering kernel is given as

$$\Lambda_{ij;kl} = -i\frac{\partial^2\Gamma_2[S]}{\partial S_{ji}\partial S_{lk}}. \quad (26)$$

In the following we will calculate $\Gamma_2[S]$ to next-to-leading order (NLO) in the expansion of $1/N_c$. The leading order (LO) and NLO terms of Γ_2 are shown diagrammatically in Figs. 1 and 2 respectively, and their expressions are given as

$$\Gamma_2^{\text{LO}}[S] = G\sum_\alpha\int d^4x\,\text{tr}(iS(x,x)\Gamma_\alpha)\text{tr}(iS(x,x)\Gamma_\alpha), \quad (27)$$

$$\Gamma_2^{\text{NLO}}[S] = \frac{i}{2}\,\text{Tr}_{c,\alpha}\ln\mathbf{B}, \quad (28)$$

with

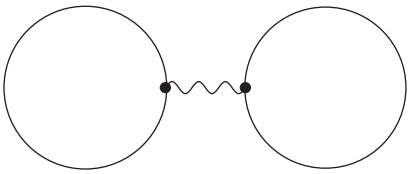

FIG. 1. Leading order (LO) contribution to Γ_2. The solid lines represent the dressed quark propagator, and the wavy line the local four-point interaction.

$$B_{\alpha_1\alpha_2}(x,y) = \delta^4(x-y)\delta_{\alpha_1\alpha_2} - 2G\Pi_{\alpha_1\alpha_2}(x,y), \quad (29)$$

$$\Pi_{\alpha_1\alpha_2}(x,y) = -i\text{tr}[iS(y,x)\Gamma_{\alpha_1}iS(x,y)\Gamma_{\alpha_2}], \quad (30)$$

where $\Pi_{\alpha_1\alpha_2}(x,y)$ are the quark-antiquark polarization functions. The scalar and pseudoscalar interaction channels correspond to $\Gamma_{\alpha=0} = \mathbb{1}$ and $\Gamma_{\alpha=a} = i\gamma_5\tau_a$, respectively. We should note that the different trace notations in the equations above have different meanings: tr only acts in the inner space (Dirac, flavor, and color), and $\text{Tr}_{c,\alpha}$ in the coordinate space and α index. Since the coupling strength $G \sim \mathcal{O}(N_c^{-1})$, it is obvious that $\Gamma_2^{\text{LO}} \sim \mathcal{O}(N_c)$ and $\Gamma_2^{\text{NLO}} \sim \mathcal{O}(1)$.

Following the method in Ref. [30], we introduce the "meson propagators" as

$$D_{\alpha_1\alpha_2}(x,y) = 2GB^{-1}_{\alpha_1\alpha_2}(x,y). \quad (31)$$

The meson propagators are related to the polarization functions through

$$D_{\alpha_1\alpha_2}(x,y) = 2G\Big[\delta_{\alpha_1\alpha_2}\delta^4(x-y) + \sum_{\alpha_3}\int d^4z\,\Pi_{\alpha_1\alpha_3}(x,z)D_{\alpha_3\alpha_2}(z,y)\Big]. \quad (32)$$

Substituting Eqs. (27) and (28) into Eqs. (23) and (26) and after a calculation which is presented in Appendix A, we obtain the expressions of self-energy and scattering kernel in the $1/N_c$ expansion in NLO. Here, we just list these results in momentum space:

$$\Sigma(p) = \Sigma^{\text{LO}}(p) + \Sigma^{\text{NLO}}(p) + \cdots, \quad (33)$$

with

$$\Sigma^{\text{LO}}(p) = 2G\int\frac{d^4q}{(2\pi)^4}\,\text{tr}(iS(q)), \quad (34)$$

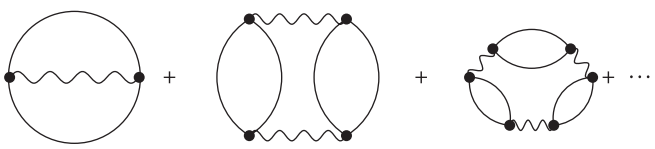

FIG. 2. NLO contribution to Γ_2.

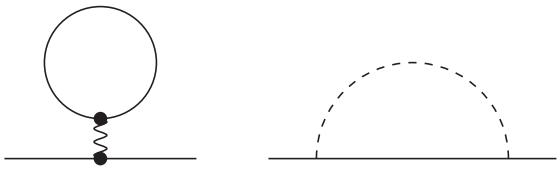

FIG. 3. Quark self-energy at LO and NLO. The dashed line denotes the meson propagator.

$$\Sigma^{\mathrm{NLO}}(p) = -\sum_{\alpha}\int\frac{d^4q}{(2\pi)^4}D_\alpha(p-q)\Gamma_\alpha iS(q)\Gamma_\alpha. \quad (35)$$

The polarization functions and meson propagators are given by

$$\Pi_\alpha(p) = -i\int\frac{d^4q}{(2\pi)^4}\,\mathrm{tr}[iS(q-p)\Gamma_\alpha iS(q)\Gamma_\alpha], \quad (36)$$

$$D_\alpha(p) = \frac{2G}{1-2G\Pi_\alpha(p)}, \quad (37)$$

Figure 3 shows the diagrams of the self-energy at LO and NLO.

The integral equation for 4-point vertex $\Gamma^{(4)}$ is given by

$$\Gamma^{(4)}_{ij;kl}(p,p';q) = \Lambda_{ij;kl}(p,p';q) - \int\frac{d^4r}{(2\pi)^4}\Lambda_{ij;k'l'}(p,r;q) \times (iS_{l'i'}(r+q))\Gamma^{(4)}_{i'j';kl}(r,p';q)(iS_{j'k'}(r)), \quad (38)$$

where the scattering kernel takes the following form:

$$\Lambda_{ij;kl}(p,r;q) = \Lambda^{\mathrm{LO}}_{ij;kl}(p,r;q) + \Lambda^{\mathrm{NLO}}_{ij;kl}(p,r;q) + \cdots, \quad (39)$$

with

$$\Lambda^{\mathrm{LO}}_{ij;kl}(p,r;q) = 2iG\sum_{\alpha}\Gamma^{\alpha}_{ij}\Gamma^{\alpha}_{kl}, \quad (40)$$

$$\Lambda^{\mathrm{NLO}}_{ij;kl}(p,r;q) = -i\sum_{\alpha}D_\alpha(p-r)\Gamma^{\alpha}_{il}\Gamma^{\alpha}_{kj} - \sum_{\alpha_1\alpha_2}\int\frac{d^4l}{(2\pi)^4} \times(\Gamma_{\alpha_1}iS(p+l)\Gamma_{\alpha_2})_{ij}D_{\alpha_1}(q-l)D_{\alpha_2}(l) \times(\Gamma_{\alpha_2}iS(r+l)\Gamma_{\alpha_1})_{kl} - \sum_{\alpha_1\alpha_2}\int\frac{d^4l}{(2\pi)^4}(\Gamma_{\alpha_1}iS(p+l)\Gamma_{\alpha_2})_{ij} \times D_{\alpha_1}(q-l)D_{\alpha_2}(l)(\Gamma_{\alpha_1}iS(r+q-l)\Gamma_{\alpha_2})_{kl}. \quad (41)$$

Figures 4 and 5 show the integral equation and NLO contributions to the scattering kernel, respectively.

III. MESON PROPAGATORS AND QUARK SELF-ENERGY

In the section we calculate the meson propagators and quark self-energy at finite temperature. We will adopt the imaginary-time, i.e., Matsubara formalism throughout this paper. In the imaginary-time formalism, the energy is replaced by discrete Matsubara frequencies $i\omega_n$ with $\omega_n = 2n\pi T$ for bosons and $\omega_n = (2n+1)\pi T$ for fermions. Furthermore, the 4-momentum integrations in the last section are replaced by

$$\int\frac{d^4p}{(2\pi)^4}f(p^0,\vec{p}) = i\beta^{-1}\sum_n\int\frac{d^3p}{(2\pi)^3}f(i\omega_n,\vec{p}), \quad (42)$$

with $\beta = 1/T$ being the inverse of the temperature.

From Eqs. (34) and (35) one finds that the LO part of the quark self-energy Σ^{LO} is of order $\mathcal{O}(1)$ in the $1/N_c$ expansion. Therefore, the real part of Σ^{NLO} can be neglected, because it is $\mathcal{O}(N_c^{-1})$. Furthermore, we should emphasize that the first nonvanishing imaginary part of the quark self-energy occurs at the order of $\mathcal{O}(N_c^{-1})$. The same also happens in the $O(N)$ model [30]. As a consequence we only need the LO part Σ^{LO} of the quark self-energy in the gap equation (22) and the polarization functions in (36),

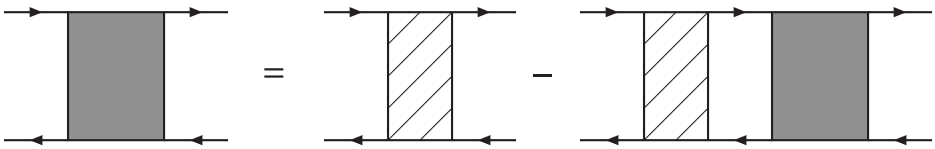

FIG. 4. Integral equation for 4-point vertex $\Gamma^{(4)}$.

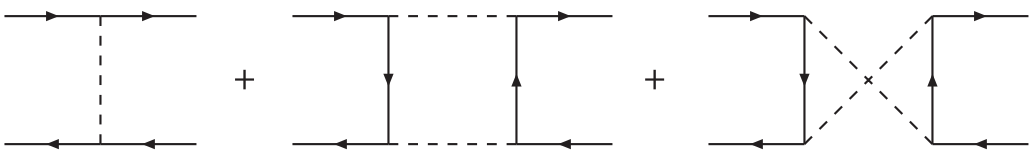

FIG. 5. NLO contributions to the 4-point scattering kernel.

which simplifies the calculations considerably. The gap equation is given by

$$M = m_0 + 4GN_cN_f \int \frac{d^3q}{(2\pi)^3}\frac{M}{E_q}(1-2n_f(E_q)), \quad (43)$$

with

$$E_q = \sqrt{q^2+M^2}, \quad (44)$$

$$n_{f,b}(E_q) = \frac{1}{e^{\beta E_q}\pm 1}, \quad (45)$$

where M is the dressed or constituent quark mass. From Eq. (36) one obtains the scalar polarization function which reads

$$\mathrm{Re}\Pi_0(p^0+i0^+,\vec{p}) = 4N_cN_f\left[I_1 + \frac{1}{2}(p_0^2-p^2-4M^2)\mathrm{Re}I(p^0+i0^+,\vec{p})\right], \quad (46)$$

$$\mathrm{Im}\Pi_0(p^0+i0^+,\vec{p}) = 2N_cN_f(p_0^2-p^2-4M^2)\mathrm{Im}I(p^0+i0^+,\vec{p}), \quad (47)$$

and the pseudoscalar polarization function

$$\mathrm{Re}\Pi_a(p^0+i0^+,\vec{p}) = 4N_cN_f\left[I_1 + \frac{1}{2}(p_0^2-p^2)\mathrm{Re}I(p^0+i0^+,\vec{p})\right], \quad (48)$$

$$\mathrm{Im}\Pi_a(p^0+i0^+,\vec{p}) = 2N_cN_f(p_0^2-p^2)\mathrm{Im}I(p^0+i0^+,\vec{p}), \quad (49)$$

with

$$I_1 = \int \frac{d^3q}{(2\pi)^3}\frac{1}{2E_q}(1-2n_f(E_q)), \quad (50)$$

$$\mathrm{Re}I(p^0+i0^+,\vec{p}) = \frac{1}{(2\pi)^2}\frac{1}{2p}\int_0^\infty dq\frac{q}{E_q} \times\left[-n_f(E_q)\ln\left|\frac{(E_+-E_q)^2-p_0^2}{(E_--E_q)^2-p_0^2}\right| + \left(\frac{1}{2}-n_f(E_q)\right)\ln\left|\frac{(E_++E_q)^2-p_0^2}{(E_-+E_q)^2-p_0^2}\right|\right], \quad (51)$$

$$\mathrm{Im}I(p^0+i0^+,\vec{p}) = -\frac{1}{16\pi}\frac{1}{p}\left\{2T\Theta(p^2-p_0^2)\ln\left(\frac{1+e^{-\sqrt{p_-^2+M^2}/T}}{1+e^{-\sqrt{p_+^2+M^2}/T}}\right) + \Theta(p_0^2-p^2-4M^2)\left[\sqrt{p_-^2+M^2}-\sqrt{p_+^2+M^2} + 2T\ln\left(\frac{1+e^{-\sqrt{p_-^2+M^2}/T}}{1+e^{-\sqrt{p_+^2+M^2}/T}}\right)\right]\right\}, \quad (52)$$

where we have

$$E_\pm = [(q\pm p)^2+M^2]^{1/2}, \quad (53)$$

$$p_\pm = \frac{1}{2}\left|p \pm p^0\sqrt{1-\frac{4M^2}{p_0^2-p^2}}\right|. \quad (54)$$

From Eq. (52) one sees that the imaginary part of the quark-antiquark polarization functions are nonvanishing only when $s<0$ ($s=p_0^2-p^2$) or $s>4M^2$. Therefore, in these regions, one can employ Eq. (37) to obtain the retarded and advanced meson propagators $D_R^\alpha(p) \equiv -D^\alpha(p^0+i0^+,\vec{p})$ and $D_A^\alpha(p) = D_R^\alpha(p)^*$. It then follows that the meson spectral density is given by

$$\rho_D^\alpha(p) = i(D_R^\alpha(p)-D_A^\alpha(p)) = \frac{8G^2\mathrm{Im}\Pi_\alpha(p^0+i0^+,\vec{p})}{(1-2G\mathrm{Re}\Pi_\alpha(p^0+i0^+,\vec{p}))^2+(2G\mathrm{Im}\Pi_\alpha(p^0+i0^+,\vec{p}))^2}. \quad (55)$$

In the region $0<s<4M^2$, we should investigate whether there is a pole in the meson propagators, in other words, whether the mass of the mesons is less than $2M$. For the pion this is fulfilled below the Mott temperature T_M, defined by

$$m_\pi(T_M) = 2M(T_M). \quad (56)$$

However, in the scalar channel, the mass of the σ meson m_σ is always larger than $2M$. (See the left panel of Fig. 6. The three parameters of the NJL model are fixed as $\Lambda = 651$ MeV, $G = 5.04$ GeV^{-2}, and $m_0 = 5.5$ MeV, which are obtained by fitting the following physical quantities: $m_\pi = 139.3$ MeV, $f_\pi = 92.3$ MeV, and $|\langle\bar{\psi}_u\psi_u\rangle|^{1/3} = 251$ MeV. Same as the usual NJL literatures, e.g. Ref. [36], we only employ the cutoff Λ for the vacuum contribution. Since the thermal contribution is finite, it does not need a regularization.) Therefore, we only need to include the single particle contribution to the spectral density for the pseudoscalar channel. In summary, the spectral density for the σ meson is given by Eq. (55), while that for the pion is changed to

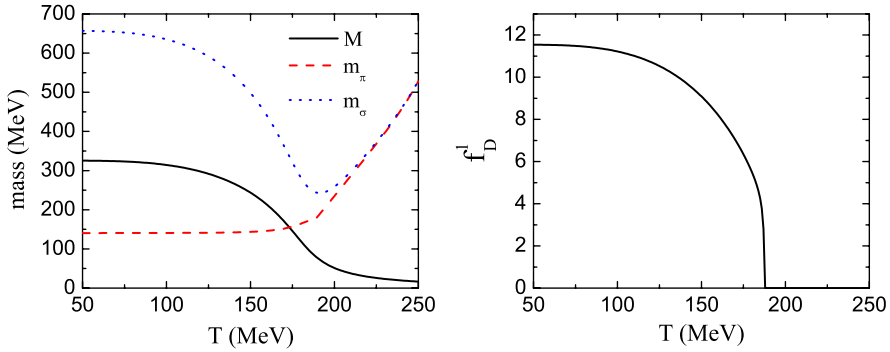

FIG. 6 (color online). Left panel: Quark constituent mass M, pion mass m_π, and σ meson mass m_σ as functions of the temperature with $|\vec{p}| = 100$ MeV. Right panel: f_{D^1} as a function of temperature with $|\vec{p}| = 100$ MeV.

$$\rho_D^1(p) = \frac{8G^2\mathrm{Im}\Pi_1}{(1-2G\mathrm{Re}\Pi_1)^2 + (2G\mathrm{Im}\Pi_1)^2} + f_D^1 2\pi \mathrm{sgn}(p_0)\delta(p_0^2 - p^2 - m_\pi^2)\Theta(2M - m_\pi), \tag{57}$$

where we use index 1 to denote the pseudoscalar channel, while f_D^1 is the residue of the pion propagator at the pole. Figure 7 shows the scalar and pseudoscalar spectral density (without the isolated single-particle contribution) for several different temperatures. One observes that there is an obvious peak in ρ_D^0, which originates from the pole of the σ meson propagator. However, in ρ_D^1, there is no such peak when the temperature is low. With increasing temperature, the isolated single-particle contribution to the spectral density becomes smaller and smaller and vanishes eventually at the Mott temperature (see the right panel of Fig. 6 which shows f_D^1 as a function of the temperature), while the continuous spectral density coming from the pole of the pion propagator becomes more and more important.

In the following, we calculate the NLO of the quark self-energy from Eq. (35) (details of the computation are presented in Appendix B and we just list the results here), whose expression in the imaginary time formalism is given by

$$\Sigma^{\mathrm{NLO}}(i\omega_{n_p}, \vec{p}) = \sum_\alpha \int \frac{d^3q}{(2\pi)^3} \beta^{-1} \sum_{n_q} D_\alpha(i\omega_{n_q} - i\omega_{n_p}, \vec{q} - \vec{p}) \Gamma_\alpha S(i\omega_{n_q}, \vec{q}) \Gamma_\alpha, \tag{58}$$

where $\omega_{n_q} = (2n_q + 1)\pi/\beta$ and $\omega_{n_p} = (2n_p + 1)\pi/\beta$. In order to complete the summation over n_q, we adopt the Holstein summation formula [37,38], i.e.,

$$\beta^{-1} \sum_{\mathrm{even,odd}m} F(i\omega_m) = \mp \sum_{\mathrm{poles}} n_{b,f}(z_i)\mathrm{Res}(F, z = z_i) \pm \sum_{\mathrm{cuts}} \int_{-\infty}^{\infty} \frac{d\xi}{2\pi i} n_{b,f}(\xi)\mathrm{Disc}F, \tag{59}$$

and find

$$\Sigma^{\mathrm{NLO}}(i\omega_{n_p}, \vec{p}) = \sum_\alpha \int \frac{d^3q}{(2\pi)^3} \int \frac{d\xi}{2\pi i} [iD_\alpha(\xi - i\omega_{n_p}, \vec{q} - \vec{p}) \Gamma_\alpha \rho_S(\xi, \vec{q}) \Gamma_\alpha n_f(\xi) + i\rho_D^\alpha(\xi, \vec{q} - \vec{p}) \Gamma_\alpha S(\xi + i\omega_{n_p}, \vec{q}) \Gamma_\alpha n_b(\xi)], \tag{60}$$

where ρ_S is the spectral density for the Hartree quark propagator

$$\rho_S(q) = 2\pi \mathrm{sgn}(q^0)\delta(q_0^2 - E_q^2)(\gamma_\mu q^\mu + M). \tag{61}$$

After analytic continuation, we arrive at

$$\mathrm{Im}\Sigma_R^{\mathrm{NLO}}(p_0, \vec{p}) = \frac{1}{2i}[\Sigma^{\mathrm{NLO}}(p_0 + i0^+, \vec{p}) - \Sigma^{\mathrm{NLO}}(p_0 - i0^+, \vec{p})] = -\frac{1}{2} \int \frac{d^4q}{(2\pi)^4} [\rho_D^+(q^0 - p^0, \vec{q} - \vec{p})(\gamma_\mu q^\mu) + \rho_D^-(q^0 - p^0, \vec{q} - \vec{p})M] \rho_G(q^0, \vec{q}) [n_f(q^0) + n_b(q^0 - p^0)], \tag{62}$$

with

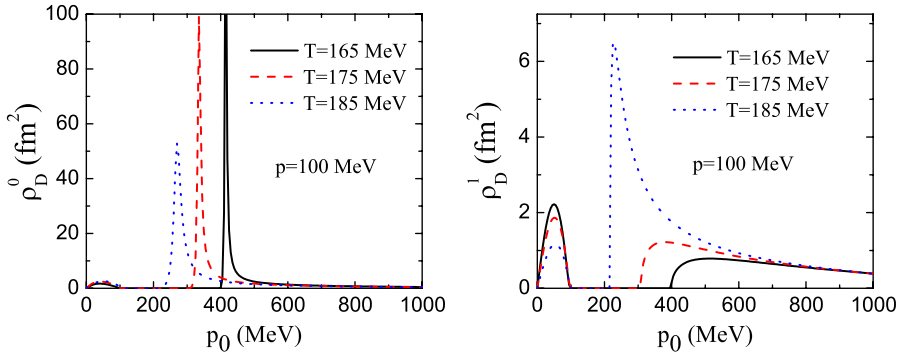

FIG. 7 (color online). σ meson (left panel) and pion (right panel) spectral densities as functions of p_0 with $|\vec{p}| = 100$ MeV at several values of the temperature.

$$\rho_G(q^0, \vec{q}) \equiv 2\pi \mathrm{sgn}(q^0)\delta(q_0^2 - E_q^2), \tag{63}$$

$$\rho_D^+(q^0, \vec{q}) = \rho_D^0(q^0, \vec{q}) + 3\rho_D^1(q^0, \vec{q}), \tag{64}$$

$$\rho_D^-(q^0, \vec{q}) = \rho_D^0(q^0, \vec{q}) - 3\rho_D^1(q^0, \vec{q}). \tag{65}$$

We express $\mathrm{Im}\Sigma_R^{\mathrm{NLO}}$ as

$$\mathrm{Im}\Sigma_R^{\mathrm{NLO}}(p_0, \vec{p}) = -\gamma^0 p^0 \mathrm{Im}C_R(p_0, \vec{p}) + \vec{\gamma}\cdot\vec{p}\,\mathrm{Im}A_R(p_0, \vec{p}) + \mathrm{Im}B_R(p_0, \vec{p}). \tag{66}$$

After some calculations, one obtains

$$\begin{aligned}\mathrm{Im}A_R(p_0, \vec{p}) = \frac{1}{32\pi^2}\frac{1}{p^3}\int_0^\infty dq\frac{q}{E_q}\int_{|q-p|}^{q+p} dkk(p^2 + q^2 - k^2)[\rho_D^+(E_q - p^0, k)(n_f(E_q) + n_b(E_q - p^0)) \\ - \rho_D^+(E_q + p^0, k)(n_f(E_q) + n_b(E_q + p^0))],\end{aligned} \tag{67}$$

$$\begin{aligned}\mathrm{Im}B_R(p_0, \vec{p}) = -\frac{1}{16\pi^2}\frac{M}{p}\int_0^\infty dq\frac{q}{E_q}\int_{|q-p|}^{q+p} dkk[\rho_D^-(E_q - p^0, k)(n_f(E_q) + n_b(E_q - p^0)) \\ - \rho_D^-(E_q + p^0, k)(n_f(E_q) + n_b(E_q + p^0))],\end{aligned} \tag{68}$$

$$\begin{aligned}\mathrm{Im}C_R(p_0, \vec{p}) = \frac{1}{16\pi^2}\frac{1}{p^0 p}\int_0^\infty dqq\int_{|q-p|}^{q+p} dkk[\rho_D^+(E_q - p^0, k)(n_f(E_q) + n_b(E_q - p^0)) \\ + \rho_D^+(E_q + p^0, k)(n_f(E_q) + n_b(E_q + p^0))].\end{aligned} \tag{69}$$

As we have mentioned above, $\mathrm{Im}\Sigma^{\mathrm{NLO}}$ is proportional to $1/N_c$. Therefore, we can approximate the quark propagator as

$$S_R(p^0, \vec{p}) \equiv \frac{\gamma\cdot p + M}{p_0^2 - \vec{p}^2 - M^2 + iF_R(p^0, \vec{p})}, \tag{70}$$

with

$$F_R(p^0, \vec{p}) = 2[p_0^2 \mathrm{Im}C_R(p_0, \vec{p}) - \vec{p}^2 \mathrm{Im}A_R(p_0, \vec{p}) - M\mathrm{Im}B_R(p_0, \vec{p})]. \tag{71}$$

We define

$$G_R(p^0, \vec{p}) \equiv G(p^0 + i0^+, \vec{p}) \equiv \frac{1}{p_0^2 - \vec{p}^2 - M^2 + iF_R(p^0, \vec{p})}. \tag{72}$$

In the following, we adopt the method in Ref. [30] and obtain the corresponding spectral density as

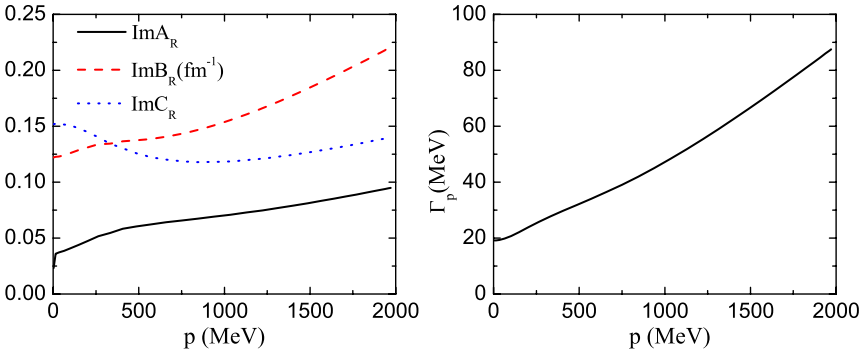

FIG. 8 (color online). Left panel: $\mathrm{Im}A_R(E_p, \vec{p})$, $\mathrm{Im}B_R(E_p, \vec{p})$, and $\mathrm{Im}C_R(E_p, \vec{p})$ as functions of $|\vec{p}|$ at $T = 130$ MeV. Right panel: Γ_p as a function of $|\vec{p}|$ at $T = 130$ MeV.

$$\rho_G(p^0, \vec{p}) = i(G_R(p^0, \vec{p}) - G_A(p^0, \vec{p})) = \frac{2F_R(p)}{(p_0^2 - E_p^2)^2 + F_R^2(p)}. \quad (73)$$

This spectral density can be approximated as its leading order contribution in the $1/N_c$ expansion, i.e., Eq. (63). In the following we usually encounter the product $G_R(p)G_A(p)$, which is of order N_c. This is because

$$G_R(p)G_A(p) = \frac{1}{(p_0^2 - E_p^2)^2 + F_R^2(p)} = \frac{\rho_G(p)}{2F_R(p)} = \frac{\rho_G(p)}{4p^0\Gamma_p}, \quad (74)$$

with

$$\Gamma_p = \frac{F_R(p^0, \vec{p})}{2p^0}\bigg|_{p^0=\pm E_p} = \frac{F_R(E_p, \vec{p})}{2E_p} \quad (75)$$

being the thermal width of a quark. $\mathrm{Im}A_R$, $\mathrm{Im}B_R$, $\mathrm{Im}C_R$, and Γ_p as functions of $|\vec{p}|$ with $T = 130$ MeV are shown in Fig. 8. One can see that the thermal width increases with $|\vec{p}|$ when the temperature is 130 MeV. In order to investigate the dependence of the thermal width on temperature, we show Γ_p as a function of T at several values of momentum in Fig. 9. In the regime of low momentum, which contributes to the shear viscosity mostly as Eq. (86) shows, we find that Γ_p has a maximal value at the pseudocritical temperature of the chiral crossover. When the momentum is high, temperature corresponding to the maximal Γ_p becomes larger.

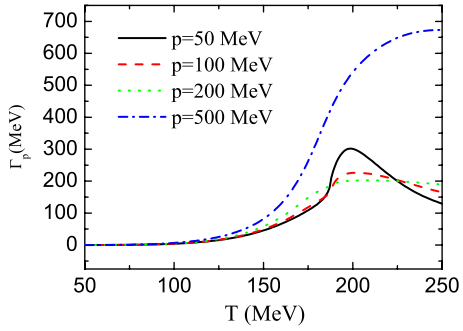

FIG. 9 (color online). Dependence of the thermal width on the temperature at several values of momentum.

IV. SHEAR VISCOSITY

According to the Kubo formula, the shear viscosity is related to the spectral density of the energy-momentum tensor through [17,39]

$$\eta = \frac{1}{20}\lim_{q^0\to 0}\lim_{\vec{q}\to 0}\frac{\partial}{\partial q^0}\rho_{TT}(q^0, \vec{q}), \quad (76)$$

with

$$\rho_{TT}(q^0, \vec{q}) = \int d^4x e^{iq^0t - i\vec{q}\cdot\vec{x}}\langle[T_{ij}(x), T_{ij}(0)]\rangle, \quad (77)$$

where T_{ij} is the traceless spatial energy-momentum tensor

$$T_{ij} = \bar{\psi}\left(i\gamma_i\partial_j - \frac{1}{3}\delta_{ij}i\gamma_k\partial_k\right)\psi. \quad (78)$$

Defining the Green function as

$$iG_{TT}(x) = \langle T(T_{ij}(x), T_{ij}(0))\rangle, \quad (79)$$

we have

$$\rho_{TT}(q^0, \vec{q}) = -2\mathrm{Im}G_{TT}(q^0 + i0^+, \vec{q}). \quad (80)$$

One easily obtains that

$$G_{TT}(q^0 = i\omega_{n_q}, 0) = \beta^{-1}\sum_{n_p}\int\frac{d^3p}{(2\pi)^3}\mathrm{Tr}[\Gamma_{ij}(p+q, p) \times S(p)\Gamma^0_{ij}(p, p+q)S(p+q)], \quad (81)$$

and the corresponding diagram is shown in Fig. 10, where Γ^0_{ij} is the bare 3-point vertex, given by

$$\Gamma^0_{ij}(p+q, p) = \gamma_i p_j - \frac{1}{3}\delta_{ij}\gamma_k p_k, \quad (82)$$

and Γ_{ij} is the fully dressed 3-point vertex. It is convenient to express Γ_{ij} as

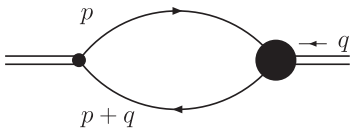

FIG. 10. Diagrammatic representation of Eq. (81), where the dot and black circle denote the bare and dressed vertices, respectively.

$$\Gamma_{ij}(p+q,p) = \Gamma^0_{ij}(p+q,p)\Gamma(p+q,p). \tag{83}$$

The dressed 3-point vertex has a relation with the 4-point vertex, which is shown in the first line of Fig. 11. Employing the Bethe-Salpeter (BS) equation for the 4-point vertex shown in Fig. 4, one obtains the BS equation for the dressed 3-point vertex as the second line of Fig. 11 shows. This is analogous to the method used by G. Aarts *et al.* to obtain the BS equation for the 3-point vertex in the $O(N)$ model [30].

Employing the Holstein summation formula in Eq. (59), we obtain

$$\begin{aligned}\lim_{q^0\to 0}\rho_{TT}(q^0,0) = \frac{32}{3}N_cN_f\beta q^0\int\frac{d^4p}{(2\pi)^4}n_f(p^0)(1-n_f(p^0))\\ \times\Gamma(p^0+q^0+i0^+,p^0-i0^+;\vec{p})\\ \times\vec{p}^2(-2M^2-\vec{p}^2+2p_0^2)G_R(p^0,\vec{p})\\ \times G_A(p^0,\vec{p}).\end{aligned} \tag{84}$$

Therefore, in order to calculate the shear viscosity one should analytically continue the 3-point vertex to

$$\mathcal{V}(p^0,\vec{p}) \equiv \Gamma_{q^0\to 0}(p^0+q^0+i0^+,p^0-i0^+;\vec{p}). \tag{85}$$

Inserting Eq. (74) into Eq. (84) and employing the Kubo formula in Eq. (76), we finally arrive at

$$\begin{aligned}\eta = \frac{1}{15\pi^2}N_cN_f\beta\int_0^\infty dp\,p^6\frac{1}{\Gamma_pE_p^2}\\ \times n_f(E_p)(1-n_f(E_p))\mathcal{V}(E_p,p).\end{aligned} \tag{86}$$

In the following, we will solve the BS equation for the dressed 3-point vertex

$$\begin{aligned}\Gamma_{xy;ij}(p+q,p) = \Gamma^0_{xy;ij}(p+q,p) - \int\frac{d^4r}{(2\pi)^4}\Lambda_{ij;k'l'}\\ \times(p,r;q)(iS_{l'i'}(r+q))\Gamma_{xy;i'j'}(r+q,r)\\ \times(iS_{j'k'}(r)),\end{aligned} \tag{87}$$

where we use x, y to denote spatial components of the energy-momentum tensor and $i, j\ldots$ the degrees of freedom in Dirac, colors, and flavors. The scattering kernel is given in Eqs. (39)–(41). Multiplying the two sides of Eq. (87) with $\gamma_x p_y$ and performing the trace, one obtains the following scalar integral equation:

$$\begin{aligned}\Gamma(p+q,p) = 1 + \int\frac{d^4r}{(2\pi)^4}\Lambda(p,r;q)\\ \times G(r+q)G(r)\Gamma(r+q,r),\end{aligned} \tag{88}$$

with

$$\Lambda(p,r;q) = \Lambda_1(p,r;q) + \Lambda_2(p,r;q) + \Lambda_3(p,r;q), \tag{89}$$

where

$$\Lambda_1(p,r;q) = i[D^0(p-r) + 3D^1(p-r)]F_0(p,r;q), \tag{90}$$

$$\begin{aligned}\Lambda_2(p,r;q) = \int\frac{d^4l}{(2\pi)^4}G(p+l)G(r+l)\{[D^0(q-l)D^0(l)\\ + 3D^1(q-l)D^1(l)]F_1(p,r,l;q)\\ + [D^0(q-l)D^0(l) - 3D^1(q-l)D^1(l)]\\ \times F_3(\vec{p},\vec{r},\vec{l})\},\end{aligned} \tag{91}$$

$$\begin{aligned}\Lambda_3(p,r;q) = \int\frac{d^4l}{(2\pi)^4}G(p+l)G(r+q-l)\{[D^0(q-l)D^0(l)\\ + 3D^1(q-l)D^1(l)]F_2(p,r,l;q)\\ + [D^0(q-l)D^0(l) - 3D^1(q-l)D^1(l)]\\ \times F_3(\vec{p},\vec{r},\vec{l})\}.\end{aligned} \tag{92}$$

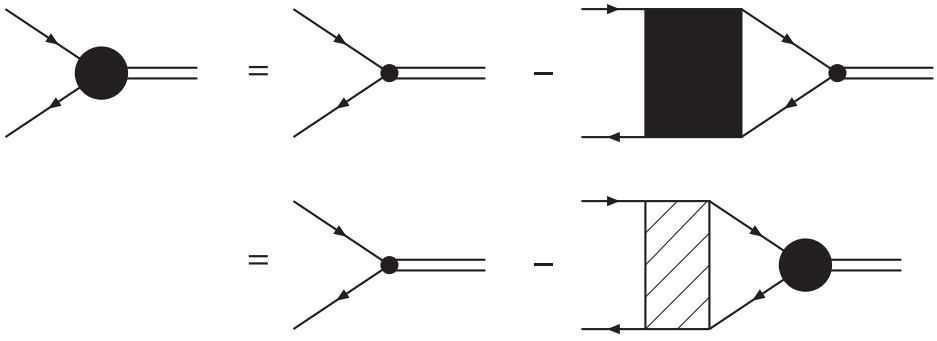

FIG. 11. Bethe-Salpeter equation for the dressed 3-point vertex and its relation with the 4-point vertex.

The three terms correspond to the three diagrams of the NLO contributions to the scattering kernel in Fig. 5, respectively. In fact, the LO scattering kernel does not contribute to Eq. (88). Some expressions included in Eqs. (90)–(92) are defined as follows:

$$F_0(p,r;q)=\frac{\vec{r}\cdot\vec{p}}{\vec{p}^2}\Big[-M^2-\frac{1}{2}\vec{r}^2+(r^0+q^0)r^0\Big], \tag{93}$$

$$\begin{aligned}F_1(p,r,l;q)=&-\frac{3}{2}\frac{N_cN_f}{\vec{p}^2}\Big\{\Big[\vec{r}\cdot\vec{p}\,\vec{r}\cdot(\vec{p}+\vec{l})-\frac{1}{3}\vec{r}^2\vec{p}\cdot(\vec{p}+\vec{l})\Big][(r^0+l^0)(2r^0+q^0)-2\vec{r}\cdot(\vec{r}+\vec{l})]\\&-\Big[\vec{r}\cdot\vec{p}(\vec{r}+\vec{l})\cdot(\vec{p}+\vec{l})-\frac{1}{3}\vec{r}\cdot(\vec{r}+\vec{l})\vec{p}\cdot(\vec{p}+\vec{l})\Big][(r^0+q^0)r^0-\vec{r}^2-M^2]\Big\},\end{aligned} \tag{94}$$

$$\begin{aligned}F_2(p,r,l;q)=&-\frac{3}{2}\frac{N_cN_f}{\vec{p}^2}\Big\{\Big[\vec{r}\cdot\vec{p}\,\vec{r}\cdot(\vec{p}+\vec{l})-\frac{1}{3}\vec{r}^2\vec{p}\cdot(\vec{p}+\vec{l})\Big][(r^0+q^0-l^0)(2r^0+q^0)-2\vec{r}\cdot(\vec{r}-\vec{l})]\\&-\Big[\vec{r}\cdot\vec{p}(\vec{r}-\vec{l})\cdot(\vec{p}+\vec{l})-\frac{1}{3}\vec{r}\cdot(\vec{r}-\vec{l})\vec{p}\cdot(\vec{p}+\vec{l})\Big][(r^0+q^0)r^0-\vec{r}^2-M^2]\Big\},\end{aligned} \tag{95}$$

$$F_3(\vec{p},\vec{r},\vec{l})=-3N_cN_f\frac{M^2}{\vec{p}^2}\Big[\vec{r}\cdot\vec{p}\,\vec{r}\cdot(\vec{p}+\vec{l})-\frac{1}{3}\vec{r}^2\vec{p}\cdot(\vec{p}+\vec{l})\Big]. \tag{96}$$

We now return to the Matsubara formalism. After performing the frequency summations with Eq. (59), we should also accomplish the following analytic continuations:

$$i\omega_{n_p}\to p^0-i0^+, \tag{97}$$

$$i\omega_{n_p}+i\omega_{n_q}\to p^0+q^0+i0^+, \tag{98}$$

$$i\omega_{n_q}\to q^0+i0^+, \tag{99}$$

due to the requirement of the vertex in Eq. (85). Then, in the limit $q^0\to 0$, one obtains

$$\mathcal{V}(p)=1+\int\frac{d^4r}{(2\pi)^4}\mathcal{V}(r)G_R(r)G_A(r)\Lambda(p,r), \tag{100}$$

with

$$\Lambda(p,r)=\Lambda_1(p,r)+\Lambda_2(p,r)+\Lambda_3(p,r), \tag{101}$$

$$\Lambda_1(p,r)=[\rho_D^0(p-r)+3\rho_D^1(p-r)]F_0(p,r)[n_f(r^0)+n_b(r^0-p^0)], \tag{102}$$

$$\begin{aligned}\Lambda_2(p,r)=&\int\frac{d^4l}{(2\pi)^4}\rho_G(p+l)\rho_G(r+l)\{[|D_R^0(l)|^2+3|D_R^1(l)|^2]F_1(p,r,l)+[|D_R^0(l)|^2-3|D_R^1(l)|^2]F_3(\vec{p},\vec{r},\vec{l})\}[n_f(l^0+p^0)\\&-n_f(l^0+r^0)][n_f(r^0)+n_b(r^0-p^0)],\end{aligned} \tag{103}$$

$$\begin{aligned}\Lambda_3(p,r)=&\int\frac{d^4l}{(2\pi)^4}\rho_G(p+l)\rho_G(r-l)\{[|D_R^0(l)|^2+3|D_R^1(l)|^2]F_2(p,r,l)+[|D_R^0(l)|^2-3|D_R^1(l)|^2]F_3(\vec{p},\vec{r},\vec{l})\}[n_f(l^0+p^0)\\&-n_f(l^0-r^0)][n_f(r^0)+n_b(r^0+p^0)],\end{aligned} \tag{104}$$

where we have $G_R(r)=G(r^0+i0^+,\vec{r})$, $G_A(r)=G(r^0-i0^+,\vec{r})$, and $F_{0,1,2}(p,r,l)=F_{0,1,2}(p,r,l;q=0)$

Inserting Eq. (74) into Eq. (100) and after some calculations, we arrive at the following integral equation:

$$\mathcal{V}(E_p,p)=1+\int_0^\infty dr\frac{\mathcal{H}(p,r)}{\Gamma_r}\mathcal{V}(E_r,r), \tag{105}$$

with

$$\mathcal{H}(p,r)=\mathcal{H}_1(p,r)+\mathcal{H}_2(p,r)+\mathcal{H}_3(p,r)+\mathcal{H}_4(p,r). \tag{106}$$

We have

$$\mathcal{H}_1(p,r)=\frac{1}{2^6\pi^2}\frac{r^4}{p^2E_r^2}\int_{|r-p|}^{r+p}dkkz_{rp}\{[\rho_D^0(E_p-E_r,k)+3\rho_D^1(E_p-E_r,k)][n_f(E_r)+n_b(E_r-E_p)] -[\rho_D^0(E_p+E_r,k)+3\rho_D^1(E_p+E_r,k)][n_f(E_r)+n_b(E_r+E_p)]\}, \tag{107}$$

with

$$z_{rp}=\frac{r^2+p^2-k^2}{2rp}; \tag{108}$$

$$\mathcal{H}_2(p,r)=-\frac{3N_cN_f}{2^8\pi^3}\frac{r}{E_r^2p^3}\int_{|r-p|}^{\infty}dl\int_{\sqrt{l^2+4M^2}}^{\infty}dl^0\left\{[|D_R^0(l)|^2+3|D_R^1(l)|^2]\left(\frac{l^2-l_0^2}{2}+M^2\right)+[|D_R^0(l)|^2-3|D_R^1(l)|^2]M^2\right\} \times\left[\left(\frac{1}{3}-z_{pl}^2-z_{rl}^2+3z_{pl}^2z_{rl}^2\right)p^2r^2+2z_{pl}\left(z_{rl}^2-\frac{1}{3}\right)r^2pl\right][n_f(l^0-E_r)-n_f(l^0-E_p)][n_f(E_r)+n_b(E_r-E_p)], \tag{109}$$

with

$$z_{pl}=\frac{l_0^2-l^2-2E_pl_0}{2pl},\qquad z_{rl}=\frac{l_0^2-l^2-2E_rl_0}{2rl}; \tag{110}$$

$$\mathcal{H}_3(p,r)=-\frac{3N_cN_f}{2^8\pi^3}\frac{r}{E_r^2p^3}\int_0^{\infty}dl\int_{-l}^{l}dl^0\left\{[|D_R^0(l)|^2+3|D_R^1(l)|^2]\left(\frac{l^2-l_0^2}{2}+M^2\right)+[|D_R^0(l)|^2-3|D_R^1(l)|^2]M^2\right\} \times\left[\left(\frac{1}{3}-z_{pl}^2-z_{rl}^2+3z_{pl}^2z_{rl}^2\right)p^2r^2+2z_{pl}\left(z_{rl}^2-\frac{1}{3}\right)r^2pl\right][n_f(l^0-E_r)-n_f(l^0-E_p)][n_f(E_r)+n_b(E_r-E_p)], \tag{111}$$

with

$$z_{pl}=\frac{l_0^2-l^2-2E_pl_0}{2pl},\qquad z_{rl}=\frac{l_0^2-l^2-2E_rl_0}{2rl}; \tag{112}$$

$$\mathcal{H}_4(p,r)=-\frac{3N_cN_f}{2^8\pi^3}\frac{r}{E_r^2p^3}\int_0^{r+p}dl\int_{-l}^{l}dl^0\left\{[|D_R^0(l)|^2+3|D_R^1(l)|^2]\left(\frac{l^2-l_0^2}{2}+M^2\right)+[|D_R^0(l)|^2-3|D_R^1(l)|^2]M^2\right\} \times\left[\left(\frac{1}{3}-z_{pl}^2-z_{rl}^2+3z_{pl}^2z_{rl}^2\right)p^2r^2+2z_{pl}\left(z_{rl}^2-\frac{1}{3}\right)r^2pl\right][n_f(l^0+E_r)-n_f(l^0-E_p)][n_f(E_r)+n_b(E_r+E_p)], \tag{113}$$

with

$$z_{pl}=\frac{l_0^2-l^2-2E_pl_0}{2pl},\qquad z_{rl}=\frac{l_0^2-l^2+2E_rl_0}{2rl}. \tag{114}$$

Here $\mathcal{H}_1$ corresponds to the first diagram in Fig. 5. In our calculations we find that the second and the third diagram in Fig. 5 contribute equally to the integral equation in Eq. (105), and $\mathcal{H}_{2,3,4}$ correspond to three different $2\leftrightarrow 2$ processes due to the box diagrams in Fig. 5 [30].

Finally, employing the expressions of $\mathcal{H}_{1,2,3,4}(p,r)$ given above, one can solve the vertex BS equation in Eq. (105) numerically. After substituting the calculated results of $\mathcal{V}(p)\equiv\mathcal{V}(E_p,p)$ into Eq. (86), we can evaluate the shear viscosity. Figure 12 shows $\mathcal{V}(p)$ as a function of p at several values of temperature. It is seen that $\mathcal{V}(p)$ increases with the temperature at high momentum, but its dependence on the temperature is weaker at low momentum.

We give the calculated result of the shear viscosity as a function of the temperature in Fig. 13. We observe that η decreases rapidly with increasing temperature during the QCD crossover from the confined hadron phase to the deconfined QGP phase. When the crossover is completed, the shear viscosity arrives at its minimum value. For higher values of T, η increases slowly.

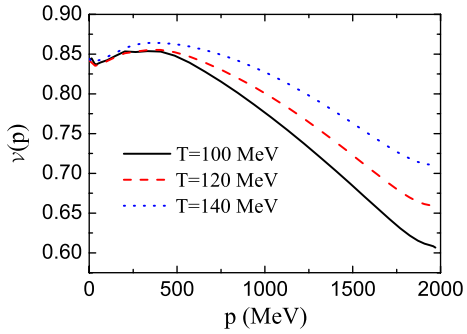

FIG. 12 (color online). $\mathcal{V}(p)$ as a function of the magnitude of the momentum p at several temperature values.

So far, we have calculated the shear viscosity in the NJL model to the first nontrivial order in the $1/N_c$ expansion. Therefore, the entropy density s also only needs to be calculated to its first nontrivial order, which has fulfilled the requirement that the ratio of the shear viscosity to entropy density η/s is calculated consistently in the $1/N_c$ expansion. The first nontrivial order of the entropy density is the mean-field LO, which can be easily obtained from the mean-field thermodynamical potential density, given by

$$\Omega(M,T) = \frac{(m_0 - M)^2}{4G} - 2N_f N_c \int \frac{d^3p}{(2\pi)^3} \times [E_p + 2T\ln(1 + e^{-\beta E_p})]. \quad (115)$$

The entropy density can be obtained by

$$s = -\frac{\partial\Omega}{\partial T}. \quad (116)$$

The numerical result of the shear viscosity to entropy density ratio η/s is shown in Fig. 14. We see that the ratio decreases monotonously with the increase of the temperature. When the temperature is above about 160 MeV, the value of η/s falls below the KPSS lower bound. η/s has also been calculated within the NJL model in the simple relaxation time approximation [40,41] and in a dynamical quasiparticle model [42]. Comparing with these calculations, we should emphasize that the present work is the first consistent

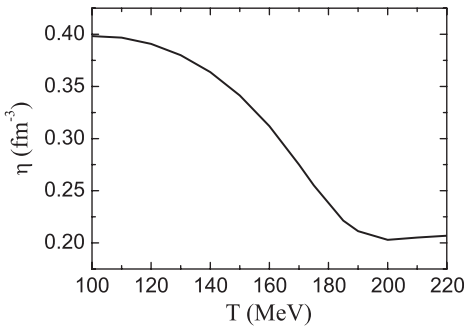

FIG. 13. Shear viscosity η as a function of the temperature.

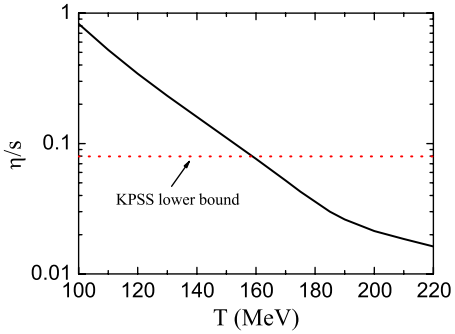

FIG. 14 (color online). Ratio of the shear viscosity to entropy density η/s as a function of the temperature. The KPSS lower bound is also shown in this plot.

computation in the $1/N_c$ expansion. Furthermore, the fully dressed 3-point vertex is also obtained from the BS equation. We find that our result lies in between Refs. [40,41] at low temperature but agrees with the latter at larger temperature. Our result also agrees with that of Ref. [42] qualitatively below the critical temperature.

V. SUMMARY AND OUTLOOK

In this work, we have calculated the temperature dependence of the shear viscosity η in the NJL model in NLO in the $1/N_c$ expansion. One has to go to this order, to obtain a description beyond the trivial mean-field LO result of a free relativistic gas. The 2PI effective action is computed at NLO, from which the integral equations for the 3- and 4-point vertex are obtained. The integral equations sum infinite sets of diagrams contributing to the shear viscosity at the same order in the $1/N_c$ expansion. The meson spectral density, self-energy and thermal width of the quarks are calculated numerically.

Our results demonstrate that η decreases rapidly when the chiral crossover is approached with increasing temperature. Compared to the hadron phase, the QGP phase has a low shear viscosity, which seems consistent with the current RHIC measurements. Furthermore, we find that the shear viscosity has a minimum value when the chiral crossover is completed and then increases slowly again. We also calculate the ratio of the shear viscosity to entropy density η/s. We find that the ratio decreases monotonously with the increase of the temperature.

Our model is a quasiparticle model. We should keep in mind that the validity of the quasiparticle model is questioned when the thermal width of a quark is large, which is the case when the temperature is high as Fig. 9 shows.

In view of the experimental search for a chiral critical end point in the QCD phase diagram in the RHIC low-energy run and the future programs at NICA/Dubna and CBM/FAIR it would be interesting to extend the present calculations to finite quark chemical potential.

ACKNOWLEDGMENTS

I am indebted to J. Wambach for useful discussions. This work was supported by the National Natural Science Foundation of China under Contract No. 11005138.

APPENDIX A: QUARK SELF-ENERGY AND SCATTERING KERNEL IN THE $1/N_c$ EXPANSION IN NLO

In this appendix we derive the expressions of quark self-energy and scattering kernel to NLO in the $1/N_c$ expansion. From Eqs. (23) and (27), the LO self-energy is easily obtained as

$$\Sigma^{\mathrm{LO}}_{ij}(x,y) = 2G\delta^4(x-y)\Gamma^{\alpha}_{ij}\mathrm{tr}(iS(x,x)\Gamma^{\alpha}). \tag{A1}$$

As for the NLO contribution, from Eq. (28) we have

$$\frac{\partial\Gamma^{\mathrm{NLO}}_2[S]}{\partial S_{ji}(y,x)} = \frac{i}{2}B^{-1}_{\alpha_1\alpha_2}(x_1,x_2)\frac{\partial B_{\alpha_2\alpha_1}(x_2,x_1)}{\partial S_{ji}(y,x)}. \tag{A2}$$

Substituting Eqs. (29) and (30), we obtain

$$\begin{aligned}\frac{\partial B_{\alpha_2\alpha_1}(x_2,x_1)}{\partial S_{ji}(y,x)} = &-2G[\Gamma^{\alpha_1}_{ii_1}iS_{i_1i_2}(x_1,x_2)\Gamma^{\alpha_2}_{i_2j}\delta^4(x_2-y)\\ &\times\delta^4(x_1-x)+\Gamma^{\alpha_2}_{ii_1}iS_{i_1i_2}(x_2,x_1)\Gamma^{\alpha_1}_{i_2j}\\ &\times\delta^4(x_1-y)\delta^4(x_2-x)].\end{aligned} \tag{A3}$$

Substituting Eq. (A3) into Eq. (A2), we arrive at

$$\frac{\partial\Gamma^{\mathrm{NLO}}_2[S]}{\partial S_{ji}(y,x)} = -2iGB^{-1}_{\alpha_1\alpha_2}(x,y)\Gamma^{\alpha_1}_{ii_1}iS_{i_1i_2}(x,y)\Gamma^{\alpha_2}_{i_2j}, \tag{A4}$$

Then the NLO self-energy is given by

$$\begin{aligned}\Sigma^{\mathrm{NLO}}_{ij}(x,y) &= -2GB^{-1}_{\alpha_1\alpha_2}(x,y)\Gamma^{\alpha_1}_{ii_1}iS_{i_1i_2}(x,y)\Gamma^{\alpha_2}_{i_2j}\\ &= -D_{\alpha_1\alpha_2}(x,y)\Gamma^{\alpha_1}_{ii_1}iS_{i_1i_2}(x,y)\Gamma^{\alpha_2}_{i_2j},\end{aligned} \tag{A5}$$

where we have used the definition of the meson propagator in Eq. (31) in the second line of the equation above. We should note that summations or integrals are assumed for all the dummy indices and arguments in the equations above.

From the definition of the four-quark scattering kernel in Eq. (26), we have

$$\begin{aligned}\Lambda_{ij;kl}(x,y;x',y') &= \frac{\partial\Sigma_{ij}(x,y)}{\partial S_{lk}(y',x')}\\ &= \frac{\partial\Sigma^{\mathrm{LO}}_{ij}(x,y)}{\partial S_{lk}(y',x')}+\frac{\partial\Sigma^{\mathrm{NLO}}_{ij}(x,y)}{\partial S_{lk}(y',x')}+\cdots.\end{aligned} \tag{A6}$$

The first term on the right-hand side of equation above is obtained as

$$\frac{\partial\Sigma^{\mathrm{LO}}_{ij}(x,y)}{\partial S_{lk}(y',x')} = 2iG\Gamma^{\alpha}_{ij}\Gamma^{\alpha}_{kl}\delta^4(x-y)\delta^4(x-y')\delta^4(x-x'); \tag{A7}$$

the second term is given by

$$\begin{aligned}\frac{\partial\Sigma^{\mathrm{NLO}}_{ij}(x,y)}{\partial S_{lk}(y',x')} = &-\frac{\partial D_{\alpha_1\alpha_2}(x,y)}{\partial S_{lk}(y',x')}\Gamma^{\alpha_1}_{ii_1}iS_{i_1i_2}(x,y)\Gamma^{\alpha_2}_{i_2j}\\ &-iD_{\alpha_1\alpha_2}(x,y)\Gamma^{\alpha_1}_{il}\Gamma^{\alpha_2}_{kj}\delta^4(x-y')\delta^4(y-x').\end{aligned} \tag{A8}$$

Furthermore, we have

$$\begin{aligned}\frac{\partial D_{\alpha_1\alpha_2}(x,y)}{\partial S_{lk}(y',x')} &= -2GB^{-1}_{\alpha_1\alpha'_1}(x,x_1)\frac{\partial B_{\alpha'_1\alpha'_2}(x_1,y_1)}{\partial S_{lk}(y',x')}B^{-1}_{\alpha'_2\alpha_2}(y_1,y)\\ &= (2G)^2B^{-1}_{\alpha_1\alpha'_1}(x,x_1)[\Gamma^{\alpha'_2}_{ki_1}iS_{i_1i_2}(y_1,x_1)\Gamma^{\alpha'_1}_{i_2l}\delta^4(x_1-y')\delta^4(y_1-x')\\ &\quad+\Gamma^{\alpha'_1}_{ki_1}iS_{i_1i_2}(x_1,y_1)\Gamma^{\alpha'_2}_{i_2l}\delta^4(y_1-y')\delta^4(x_1-x')]B^{-1}_{\alpha'_2\alpha_2}(y_1,y)\\ &= D_{\alpha_1\alpha'_1}(x,y')\Gamma^{\alpha'_2}_{ki_1}iS_{i_1i_2}(x',y')\Gamma^{\alpha'_1}_{i_2l}D_{\alpha'_2\alpha_2}(x',y)+D_{\alpha_1\alpha'_1}(x,x')\Gamma^{\alpha'_1}_{ki_1}iS_{i_1i_2}(x',y')\Gamma^{\alpha'_2}_{i_2l}D_{\alpha'_2\alpha_2}(y',y).\end{aligned} \tag{A9}$$

Substituting Eq. (A9) into Eq. (A8), we obtain

$$\begin{aligned}\frac{\partial\Sigma^{\mathrm{NLO}}_{ij}(x,y)}{\partial S_{lk}(y',x')} = &-iD_{\alpha_1\alpha_2}(x,y)\Gamma^{\alpha_1}_{il}\Gamma^{\alpha_2}_{kj}\delta^4(x-y')\delta^4(y-x')-\Gamma^{\alpha_1}_{ii_3}iS_{i_3i_4}(x,y)\Gamma^{\alpha_2}_{i_4j}[D_{\alpha_1\alpha'_2}(x,y')D_{\alpha'_1\alpha_2}(x',y)\\ &+D_{\alpha_1\alpha'_1}(x,x')D_{\alpha'_2\alpha_2}(y',y)]\Gamma^{\alpha'_1}_{ki_1}iS_{i_1i_2}(x',y')\Gamma^{\alpha'_2}_{i_2l},\end{aligned} \tag{A10}$$

which are the NLO contributions to the four-quark scattering kernel shown in Fig. 5.

APPENDIX B: NLO QUARK SELF-ENERGY

The expression of the NLO quark self-energy is given by

$$\Sigma^{\mathrm{NLO}}(i\omega_{n_p},\vec{p}) = \sum_\alpha \int \frac{d^3q}{(2\pi)^3}\beta^{-1}\sum_{n_q} D_\alpha(i\omega_{n_q}-i\omega_{n_p},\vec{q}-\vec{p})\Gamma_\alpha S(i\omega_{n_q},\vec{q})\Gamma_\alpha. \tag{B1}$$

Employing the Holstein summation formula in Eq. (59), we have

$$\begin{aligned}\beta^{-1}\sum_{n_q} D_\alpha(i\omega_{n_q}-i\omega_{n_p},\vec{q}-\vec{p})\Gamma_\alpha S(i\omega_{n_q},\vec{q})\Gamma_\alpha &= -\int_{-\infty}^{\infty}\frac{d\xi}{2\pi i} D_\alpha(\xi-i\omega_{n_p},\vec{q}-\vec{p})\Gamma_\alpha[S(\xi+i0^+,\vec{q})\\ &\quad - S(\xi-i0^+,\vec{q})]\Gamma_\alpha n_f(\xi) - \int_{-\infty}^{\infty}\frac{d\xi}{2\pi i}[D_\alpha(\xi+i0^+,\vec{q}-\vec{p})\\ &\quad - D_\alpha(\xi-i0^+,\vec{q}-\vec{p})]\Gamma_\alpha S(\xi+i\omega_{n_p},\vec{q})\Gamma_\alpha n_f(\xi+i\omega_{n_p})\\ &= \int_{-\infty}^{\infty}\frac{d\xi}{2\pi i}[iD_\alpha(\xi-i\omega_{n_p},\vec{q}-\vec{p})\Gamma_\alpha\rho_S(\xi,\vec{q})\Gamma_\alpha n_f(\xi)\\ &\quad + i\rho_D^\alpha(\xi,\vec{q}-\vec{p})\Gamma_\alpha S(\xi+i\omega_{n_p},\vec{q})\Gamma_\alpha n_b(\xi)],\end{aligned} \tag{B2}$$

where in the last step we have used the following relations:

$$\rho_S(\xi,\vec{q}) = i[S(\xi+i0^+,\vec{q}) - S(\xi-i0^+,\vec{q})], \tag{B3}$$

$$\rho_D^\alpha(\xi,\vec{q}-\vec{p}) = -i[D_\alpha(\xi+i0^+,\vec{q}-\vec{p}) - D_\alpha(\xi-i0^+,\vec{q}-\vec{p})], \tag{B4}$$

$$n_f(\xi+i\omega_{n_p}) = -n_b(\xi). \tag{B5}$$

ρ_S and ρ_D^α are the spectral densities for the quark and meson, respectively. n_b is the Bose distribution function. Substituting Eq. (B2) into Eq. (B1), we obtain

$$\begin{aligned}\Sigma^{\mathrm{NLO}}(i\omega_{n_p},\vec{p}) = \sum_\alpha\int\frac{d^3q}{(2\pi)^3}\int\frac{d\xi}{2\pi i}[iD_\alpha(\xi-i\omega_{n_p},\vec{q}-\vec{p})\Gamma_\alpha\rho_S(\xi,\vec{q})\Gamma_\alpha n_f(\xi)\\ + i\rho_D^\alpha(\xi,\vec{q}-\vec{p})\Gamma_\alpha S(\xi+i\omega_{n_p},\vec{q})\Gamma_\alpha n_b(\xi)].\end{aligned} \tag{B6}$$

Then we perform the following analytic continuation:

$$\begin{aligned}\mathrm{Im}\Sigma_R^{\mathrm{NLO}}(p_0,\vec{p}) &= \frac{1}{2i}[\Sigma^{\mathrm{NLO}}(p_0+i0^+,\vec{p}) - \Sigma^{\mathrm{NLO}}(p_0-i0^+,\vec{p})]\\ &= -\frac{1}{2}\sum_\alpha\int\frac{d^3q}{(2\pi)^3}\int\frac{d\xi}{2\pi}\{[iD_\alpha(\xi-p_0-i0^+,\vec{q}-\vec{p}) - iD_\alpha(\xi-p_0+i0^+,\vec{q}-\vec{p})]\Gamma_\alpha\rho_S(\xi,\vec{q})\Gamma_\alpha n_f(\xi)\\ &\quad + \rho_D^\alpha(\xi,\vec{q}-\vec{p})\Gamma_\alpha[iS(\xi+p_0+i0^+,\vec{q}) - iS(\xi+p_0-i0^+,\vec{q})]\Gamma_\alpha n_b(\xi)\}\\ &= -\frac{1}{2}\sum_\alpha\int\frac{d^3q}{(2\pi)^3}\int\frac{d\xi}{2\pi}\{\rho_D^\alpha(\xi-p_0,\vec{q}-\vec{p})\Gamma_\alpha\rho_S(\xi,\vec{q})\Gamma_\alpha n_f(\xi) + \rho_D^\alpha(\xi,\vec{q}-\vec{p})\Gamma_\alpha\rho_S(\xi+p_0,\vec{q})\Gamma_\alpha n_b(\xi)\}\\ &= -\frac{1}{2}\sum_\alpha\int\frac{d^3q}{(2\pi)^3}\int\frac{d\xi}{2\pi}\{\rho_D^\alpha(\xi-p_0,\vec{q}-\vec{p})\Gamma_\alpha\rho_S(\xi,\vec{q})\Gamma_\alpha n_f(\xi)\\ &\quad + \rho_D^\alpha(\xi-p_0,\vec{q}-\vec{p})\Gamma_\alpha\rho_S(\xi,\vec{q})\Gamma_\alpha n_b(\xi-p_0)\}\\ &= -\frac{1}{2}\sum_\alpha\int\frac{d^4q}{(2\pi)^4}\{\rho_D^\alpha(q_0-p_0,\vec{q}-\vec{p})\Gamma_\alpha\rho_S(q_0,\vec{q})\Gamma_\alpha[n_f(q_0)+n_b(q_0-p_0)]\},\end{aligned} \tag{B7}$$

where in the last step we have changed the integral variable ξ to q_0. Employing the spectral density of the Hartree quark propagator in Eq. (61) and defining

$$\rho_G(q^0,\vec{q}) \equiv 2\pi\mathrm{sgn}(q^0)\delta(q_0^2-E_q^2), \tag{B8}$$

as shown in Eq. (63), we have

$$\sum_\alpha \rho_D^\alpha(q_0-p_0,\vec{q}-\vec{p})\Gamma_\alpha\rho_S(q_0,\vec{q})\Gamma_\alpha = \rho_D^0(q_0-p_0,\vec{q}-\vec{p})\rho_G(q^0,\vec{q})(\gamma_\mu q^\mu + M) + 3\rho_D^1(q_0-p_0,\vec{q}-\vec{p})\rho_G(q^0,\vec{q})(\gamma_\mu q^\mu - M) = [\rho_D^0(q_0-p_0,\vec{q}-\vec{p})(\gamma_\mu q^\mu + M) + 3\rho_D^1(q_0-p_0,\vec{q}-\vec{p})(\gamma_\mu q^\mu - M)]\rho_G(q^0,\vec{q}) = \{[\rho_D^0(q_0-p_0,\vec{q}-\vec{p}) + 3\rho_D^1(q_0-p_0,\vec{q}-\vec{p})](\gamma_\mu q^\mu) + [\rho_D^0(q_0-p_0,\vec{q}-\vec{p}) - 3\rho_D^1(q_0-p_0,\vec{q}-\vec{p})]M\}\rho_G(q^0,\vec{q}). \tag{B9}$$

Substituting Eq. (B9) into Eq. (B7), we arrive at

$$\mathrm{Im}\Sigma_R^{\mathrm{NLO}}(p_0,\vec{p}) = -\frac{1}{2}\int\frac{d^4q}{(2\pi)^4}[\rho_D^+(q^0-p^0,\vec{q}-\vec{p})(\gamma_\mu q^\mu) + \rho_D^-(q^0-p^0,\vec{q}-\vec{p})M]\rho_G(q^0,\vec{q})[n_f(q^0) + n_b(q^0-p^0)], \tag{B10}$$

with ρ_D^+ and ρ_D^- defined in Eqs. (64) and (65).

We parametrize $\mathrm{Im}\Sigma$ like this:

$$\mathrm{Im}\Sigma_R^{\mathrm{NLO}}(p_0,\vec{p}) = -\gamma^0 p^0 \mathrm{Im}C_R(p_0,\vec{p}) + \vec{\gamma}\cdot\vec{p}\,\mathrm{Im}A_R(p_0,\vec{p}) + \mathrm{Im}B_R(p_0,\vec{p}). \tag{B11}$$

It then follows that

$$\mathrm{Im}A_R(p_0,\vec{p}) = \frac{1}{2p^2}\int\frac{d^4q}{(2\pi)^4}\rho_D^+(q^0-p^0,\vec{q}-\vec{p})(\vec{p}\cdot\vec{q})\rho_G(q^0,\vec{q})[n_f(q^0) + n_b(q^0-p^0)], \tag{B12}$$

$$\mathrm{Im}B_R(p_0,\vec{p}) = -\frac{M}{2}\int\frac{d^4q}{(2\pi)^4}\rho_D^-(q^0-p^0,\vec{q}-\vec{p})\rho_G(q^0,\vec{q})[n_f(q^0) + n_b(q^0-p^0)], \tag{B13}$$

$$\mathrm{Im}C_R(p_0,\vec{p}) = \frac{1}{2p_0}\int\frac{d^4q}{(2\pi)^4}\rho_D^+(q^0-p^0,\vec{q}-\vec{p})q^0\rho_G(q^0,\vec{q})[n_f(q^0) + n_b(q^0-p^0)]. \tag{B14}$$

After an easy calculation, one obtains Eqs. (67)–(69).

[1] E. V. Shuryak, Prog. Part. Nucl. Phys. **53**, 273 (2004).
[2] M. Gyulassy and L. McLerran, Nucl. Phys. **A750**, 30 (2005).
[3] E. V. Shuryak, Nucl. Phys. **A750**, 64 (2005).
[4] I. Arsene *et al.*, Nucl. Phys. **A757**, 1 (2005).
[5] B. B. Back *et al.*, Nucl. Phys. **A757**, 28 (2005).
[6] J. Adams *et al.*, Nucl. Phys. **A757**, 102 (2005).
[7] K. Adcox *et al.*, Nucl. Phys. **A757**, 184 (2005).
[8] J.-P. Blaizot, J. Phys. G **34**, S243 (2007).
[9] G. Policastro, D. T. Son, and A. O. Starinets, Phys. Rev. Lett. **87**, 081601 (2001); P. K. Kovtun, D. T. Son, and A. O. Starinets, Phys. Rev. Lett. **94**, 111601 (2005).
[10] P. Romatschke and U. Romatschke, Phys. Rev. Lett. **99**, 172301 (2007).
[11] U. W. Heinz and H. Song, J. Phys. G **35**, 104126 (2008).
[12] H. Song, S. A. Bass, U. Heinz, T. Hirano, and C. Shen, Phys. Rev. Lett. **106**, 192301 (2011); **109**, 139904(E) (2012); Phys. Rev. C **83**, 054910 (2011); **86**, 059903(E) (2012).
[13] P. Arnold, G. D. Moore, and L. G. Yaffe, J. High Energy Phys. 11 (2000) 001; 01 (2003) 030(E); 05 (2003) 051(E).
[14] G. D. Moore, J. High Energy Phys. 05 (2001) 039.
[15] Z. Xu and C. Greiner, Phys. Rev. Lett. **100**, 172301 (2008).
[16] J.-W. Chen, H. Dong, K. Ohnishi, and Q. Wang, Phys. Lett. B **685**, 277 (2010).
[17] S. Jeon, Phys. Rev. D **52**, 3591 (1995).
[18] E. Wang and U. Heinz, Phys. Rev. D **67**, 025022 (2003).
[19] H. B. Meyer, Phys. Rev. D **76**, 101701(R) (2007).
[20] P. Petreczky, J. Phys. G **35**, 044033 (2008).
[21] M. Brigante, H. Liu, R. C. Myers, S. Shenker, and S. Yaida, Phys. Rev. D **77**, 126006 (2008); Phys. Rev. Lett. **100**, 191601 (2008).
[22] A. Jakovac, Phys. Rev. D **81**, 045020 (2010).
[23] T. D. Cohen, Phys. Rev. Lett. **99**, 021602 (2007).
[24] T. D. Lee and C. N. Yang, Phys. Rev. **117**, 22 (1960).
[25] J. M. Luttinger and J. C. Ward, Phys. Rev. **118**, 1417 (1960); G. Baym and L. P. Kadanoff, Phys. Rev. **124**, 287 (1961); P. Martin and C. De Dominicis, J. Math. Phys. (N.Y.) **5**, 14 (1964); **5**, 31 (1964).
[26] J. M. Cornwall, R. Jackiw, and E. Tomboulis, Phys. Rev. D **10**, 2428 (1974).

[27] J. P. Blaizot, E. Iancu, and A. Rebhan, Phys. Rev. Lett. **83**, 2906 (1999); J. Berges, Sz. Borsányi, U. Reinosa, and J. Serreau, Phys. Rev. D **71**, 105004 (2005).
[28] J. Berges and J. Cox, Phys. Lett. B **517**, 369 (2001); G. Aarts and J. Berges, Phys. Rev. Lett. **88**, 041603 (2002); G. Aarts, D. Ahrensmeier, R. Baier, J. Berges, and J. Serreau, Phys. Rev. D **66**, 045008 (2002).
[29] J. P. Blaizot, J. M. Pawlowski, and U. Reinosa, Phys. Lett. B **696**, 523 (2011).
[30] G. Aarts and J. M. Martínez Resco, J. High Energy Phys. 02 (2004) 061.
[31] M. E. Carrington and E. Kovalchuk, Phys. Rev. D **81**, 065017 (2010).
[32] Y. Nambu and G. Jona-Lasinio, Phys. Rev. **122**, 345 (1961); **124**, 246 (1961).
[33] M. K. Volkov, Ann. Phys. (N.Y.) **157**, 282 (1984); S. P. Klevansky, Rev. Mod. Phys. **64**, 649 (1992); T. Hatsuda and T. Kunihiro, Phys. Lett. **145B**, 7 (1984); Phys. Rep. **247**, 221 (1994); M. Buballa, Phys. Rep. **407**, 205 (2005).
[34] V. Dmitrasinovic, H.-J. Schulze, R. Tegen, and R. H. Lemmer, Ann. Phys. (N.Y.) **238**, 332 (1995).
[35] M. Oertel, M. Buballa, and J. Wambach, Nucl. Phys. **A676**, 247 (2000).
[36] K. Fukushima, M. Ruggieri, and R. Gatto, Phys. Rev. D **81**, 114031 (2010).
[37] T. Holstein, Ann. Phys. (N.Y.) **29**, 410 (1964).
[38] M. A. Valle Basagoiti, Phys. Rev. D **66**, 045005 (2002).
[39] L. P. Kadanoff and P. C. Martin, Ann. Phys. (N.Y.) **24**, 419 (1963).
[40] C. Sasaki and K. Redlich, Nucl. Phys. **A832**, 62 (2010).
[41] S. Plumari, V. Baran, M. Di Toro, G. Ferini, and V. Greco, Phys. Lett. B **689**, 18 (2010).
[42] V. Ozvenchuk, O. Linnyk, M. I. Gorenstein, E. L. Bratkovskaya, and W. Cassing, Phys. Rev. C **87**, 064903 (2013).